Hindawi
International Journal of Photoenergy
Volume 2021, Article ID 6681084, 11 pages
https://doi.org/10.1155/2021/6681084

Research Article

Technoeconomic Performance Analysis of Solar Tracking Methods for Roof-Type Solar Power Plants and Electric Vehicle Charging Stations

Tahsin Boyekin[1] **and İsmail Kıyak**[2]

[1]*Department of Electrical and Electronics Engineering, Institute of Pure and Applied Sciences, Marmara University, Istanbul, Turkey*
[2]*Department of Electrical and Electronics Engineering, Faculty of the Technology, Marmara University, Istanbul, Turkey*

Correspondence should be addressed to Tahsin Boyekin; tahsinboyekin@marun.edu.tr

Received 13 November 2020; Revised 8 March 2021; Accepted 11 March 2021; Published 7 April 2021

Academic Editor: Hafiz Muhammad Ali

In building integrated photovoltaic (BIPV) solar energy projects, cost effectiveness, durability, and long-term reliability are among the criteria that should be taken into consideration as well as the gain in electricity generation efficiency. Also, in a study, it is stated that a dual-axis solar tracking system occupies approximately 100% more space than a single-axis system and 160% more than a fixed-angle system. It has been observed that most of the studies that are mounted on the building and include a tracking system are small-scale experimental studies. The aim of this article is to present a systematic analysis with a low investment cost, a low operating cost, and high reliability, in a real application especially for roof applications in buildings. Three buildings in the same location and with the same roof area were selected. Photovoltaic power plants with 23.68 kW power were installed; these panels had three types: fixed-angle, manually controlled, and single-axis solar tracking systems. The energy generation system is connected to the network with a double-sided meter, and there is a double-sided energy flow. The energy produced is used to meet the energy needs of the vehicle charging station and common areas of the buildings. Although the single-axis tracking system is 27.85% more efficient than other energy generation methods, the manually adjusted method has proven to have the shortest amortization time. The study also presents shading, which is a serious problem in large-scale roof projects, and the area covered by the module per unit watt produced.

1. Introduction

Solar power plants (SPPs) convert sunlight into electrical energy. The intensity of solar power outside the atmosphere is approximately 1370 W/m^2. However, much of this is lost due to the atmosphere, and the intensity of the solar power that reaches the Earth's surface varies between 0 and 1100 W/m^2 [1]. However, even a small portion of the remaining energy is considerably higher than the existing energy requirements [2]. Studies on solar energy have accelerated since the 1970s; photovoltaic (PV) technology is now widespread, offering increased efficiency and decreased production costs relative to fossil fuels [3]. Solar energy is also unlimited, making it better able to meet the increasing demands for energy [4–6]. Solar cells form modules with a certain number of serial or parallel connections. These modules make up arrays (also with a certain number of serial or parallel connections), and these arrays in turn comprise SPPs. There are many types of cells in PV modules [7–12]:

(i) Crystalline and multicrystalline silicon solar cells

(ii) Thin-film solar cells (a-Si, cadmium telluride, and CIS)

(iii) Nanotechnology-based solar cells (tandem, super tandem, and intermediate-band solar cells, etc.)

The most frequently used types are crystalline silicon, cadmium telluride, and CIS/CIGS cells [3]. The types of SPPs vary according to their structure. Each has various applications,

including single-axis and dual-axis solar tracking systems; roof, field, and facade applications; and grid-tied and off-grid connections [13–20]. Grid-tied SPPs can be high-power (>1-MW) systems, but their use as low-power systems in buildings is also common. These grid-tied systems can receive energy from the grid when required and can also provide excess energy to feed the grid [21]. Grid-tied systems do not need energy storage; it is sufficient to convert direct current (DC) electricity into alternating current (AC) electricity with the help of an inverter so as to conform to the [22–25]. However, nonlinear voltage waves and harmonics occur in such systems. The mathematical form of these nonlinear waves is determined using Fourier series.

Solar energy is used to generate electricity in all areas where electricity is available. PV modules are sometimes utilized for visual comfort and for the shade that they provide, in addition to their energy production [26–29]. Building-based applications were used in this project. SPPs that are usually installed on the roofs of buildings can also be installed on facades. In one developing technology, semitransparent solar modules can be installed instead of glass in some applications, although these modules have low efficiency [30–34]. Furthermore, some solar panels can be used in place of shutters; energy production can be increased by adding a solar-tracking system to these shutters [5].

Shading is the most important consideration in projections for rooftop SPPs. The amount of shade that can appear on the part of the building where the SPP will be installed should be analysed. Other building that are close to the SPP (especially taller ones) and other rooftop structures should also accounted for [35]. The shading analysis involves modelling these structures using a simulation program such as PVSyst or PV*SOL [36]. The results describe the percentage shade for each module. The modules with high shading should be replaced with modules that would be exposed to more light. In this project, these analyses were performed using the PV*SOL program [37–41].

The basic criteria to be considered in building-integrated solar energy systems can be listed as follows: solar tracking system cost, installation cost, logistics cost, space usage, operation and maintenance cost, tracking system power consumption, performance and energy gain, tracking method's solar tracking accuracy, service life, and resistance to wind and other natural abrasives. In a study where the system was installed at a latitude angle of 36.25°N, it was determined that a dual-axis solar tracking system was able to generate approximately 30% more energy than a fixed-angle system, but the area covered was approximately 100% more than a single-axis tracker and approximately 160% more than a fixed-angle system [42]. The results of another experimental study show that the total energy consumption of the single-axis tracking system is approximately 2-8% of the energy produced by the grid-connected PV system and approximately 5-12% in the dual-axis solar tracking system [43]. In this respect, when compared to building-mounted solar energy generation systems ground projects, it can be stated that project logistics, installation cost, operating cost, overall efficiency, and service life are the factors that should be paid more attention to. The aim of this study is to perform analysis on a real-time project with optimal efficiency that adopts low investment and operating costs that can be applied on building roofs, as opposed to tracking systems using various solar tracking methods including double-axis (two axis of rotation for better efficiency), hybrid model (includes both sensors and data/time to analyse the best position), polar-aligned single-axis (the tilted axis is aligned to the polar star), and azimuth/tilt roll mechanism (the ground is called azimuth axis) [22].

The main contributions of this study to the literature are as follows:

(1) In an area of approximately 1000 m^2, three different methods have been tested. This is the first academic study to be carried with a roof this size

(2) This is the most innovative approach that presents detailed cost analysis and depreciation periods among the large-scale rooftop projects

(3) This is an original study in terms of the application of minimum shading and maximum use of space among roof-mounted applications

(4) The study also provides the instantaneous monitoring of the theoretical and application performances of the system and the control of its economic feasibility

Other chapters of this paper are organized as follows: Section 2 presents a theoretical model analysis. Section 3 presents the details of the project that was implemented. Design components, energy production/consumption estimates, and application information are explained in detail. Section 4 presents the electrical system performance and cost analysis. And lastly, Section 5 provides study results and recommendations.

2. Literature Overview

In Ref. [44], researchers have compared the thermal energy produced at a specific solar position with the energy demanded and implemented a solar tracking system that determines the solar position for the new state. In Ref. [22] review study, various solar tracking system methods including single-axis, dual-axis, polar-axis, open-loop, closed-loop, hybrid model, and azimuth/tilt roll mechanism were discussed and compared with existing solar tracking methods. In Ref. [45], a dual-axis solar tracking system was designed by using the sensor information and control technologies of the solar cell to increase the overall efficiency of the PV system. In Ref. [46], three angles to the sun were estimated by predicting the position of the sun during the day. In practice, when well-calibrated, results showing an improvement between 5 and 7% were obtained.

In Ref. [47], a review of the properties and functions of systems such as building-integrated concentrating photovoltaics (BICPV), building-integrated concentrating solar thermal (BICST), and building-integrated concentrating solar daylighting (BICSD), and BICPV/T, BICPV/D, BICST/D, and BICPV/T/D are presented. In Ref. [48], a PV system was

integrated into the facade of a high-rise building and Honeybee and Ladybug were used for the first time in this study as control logic, and 354734.7 kWh/year energy was produced. In Ref. [43], using the single-axis PV tracking system, it was determined that the total energy production increased up to 30.3% for a sunny day and 15.2% in average weather conditions. In Ref. [42], the study reports a design and industrial prototype of a large-scale dual-axis solar tracker consisting of a vertical axis moving platform and multirow elevation structures. In Ref. [49], the design options for PV structural cell types are investigated and the analysis of design options for BIPV systems using an electrical-module layout with additional interlayers are presented. In Ref. [50], although the choice of trackers depended mainly on the physical characteristics of the terrain, overall, this system has proven to be more efficient and advantageous than its single-axis and fixed counterparts.

In Ref. [51], the results show that the BIPV model can estimate the average daily energy efficiency of 6.2% and the temperature behind the module with an average difference of 1.74°C. In Ref. [52], a four-position controlled vertical axis method was used and it was observed that the overall efficiency increased by 2% in the experimental solar tracking prototype study. In Ref. [53], it was observed that the solar panel production efficiency increased up to 40% in the experimental application with 4 LDR sensors and Arduino controlled application. In Ref. [54], analyses with and without thermal absorbers were performed by using a three-dimensional combined heat transfer model to increase the efficiency of the PV module.

3. Background Theory

This section gives detailed analysis of PV modules' electrical performance, irradiation modeling, and array sizing.

3.1. PV Module Analysis and Irradiance Modelling. In this section, evaluations about the electrical components of a PV module are made. Some of these parameters can be represented as short-circuit current, open-circuit current under distinct radiation conditions, and array temperature. PV cell operating temperature is different from ambient temperature and also defines open-circuit voltage. Since the cell operating temperature changes depending on the ambient temperature and solar radiation, it can be calculated using Equation (1). Equations (3), (4), and (5) are used to predict PV open-circuit voltage, current, and power, respectively [55].

$$T_c = T_a + 0.03.H_T, \tag{1}$$

$$H_T = H_b R_b + H_d R_d + (H_b + H_d) R_r, \tag{2}$$

$$V_{oc} = V_{oc,0} + \left(-\frac{2.3\text{mV}}{C}\right)(T_c - T_a), \tag{3}$$

$$I = I_{PV} - I_0\left[e^{\left(\frac{V+R_s.I}{aV_t}\right)} - 1\right] - \frac{V + R_s.I}{R_p}, \tag{4}$$

$$P_{PV} = k_1 H_T A\left[1 + k_2\left(T_a - T_a'\right)\right], \tag{5}$$

where T_c is the cell operating temperature, T_a is the ambient temperature, I_{PV} is the PV current, I_0 is the reverse current, α is a diode constant, V_t is the thermal voltage, R_p and R_s are the parallel and series equivalent resistances of the module, ε is the PV conversion rate, A is the PV surface area, H_t is the hourly PV power output (kWh/m^2), H_b is the beam radiation, H_d is the scattered radiation, and R_b, R_d, and R_r are the tilt elements for the beam, scattered, and reflected irradiation; k_1 refers to the typical distribution of modules and relevant data for a panel is included 0.095 to 0.105; and $k_2 = -0.47\%/°\text{C}$.

Irradiance collected on a photovoltaic panel surface, I_t (W/m^2), can be expressed as

$$I_t = I_f + I_r, \tag{6}$$

where I_f (W/m^2) and I_r (W/m^2) is the expression that gives the radiation reaching the front and rear parts of the photovoltaic panel, respectively. I_r is included in the formulation only when bifacial modules are used. I_f can be explained as

$$I_f = I_{dir,f} + I_{dif,f} + I_{gnd,f}, \tag{7}$$

where $I_{dir,f}$ (W/m^2),$I_{dif,f}$ (W/m^2), and$I_{gnd,f}$ (W/m^2) is the expression that gives the sum of the direct, scattered, and reflected radiation reaching the front of the photovoltaic panel. Expressions can be defined as

$$I_{dir,f} = \text{DNI}.\cos\left(A0I_f\right), \tag{8}$$

where DNI (W/m^2) is the linear irradiance and $(A0I_f)$ (°) is the angel of ratio between DNI and the normal of the photovoltaic panel front surface.

$$I_{dif,f} = \text{DHI}.\left[(1 - F_1).\frac{1 + \cos(\theta_m)}{2} + F_1.\frac{a'}{c'} + |F_2.\sin(\theta_m)|\right], \tag{9}$$

where DHI (W/m^2) is the scattered horizontal irradiance, (θ_m) (°) is the module tilt angle F_1, F_2, a' and c' are parameter characterize in following the Perez model [54]. This approach explains the celestial hemisphere in three different parts, the sky (as the first part), circumsolar (as the second part), and horizon (as the third part) can be obtain from Equation (9).

$$I_{gnd,f} = \text{GHI}.\rho.\frac{1 - \cos(\theta_m)}{2}. \tag{10}$$

Equation (10) expresses the addition of irradiation reflected from the ground according to the isotropic model. At the same time, the stated ratio will increase with GHI (W/m^2) and ground albedo, ρ during periods of high spherical horizontal radiation, as this will add to the total radiation reflected from the ground [54].

3.2. PV Array Sizing. A PV array consists of photovoltaic panels with series and parallel connected photovoltaic cells, DC to DC converters, controllers, and batteries.

The main purpose of the solar energy project is to feed the system without the need for an electricity grid. PV array calculation that will produce energy equal to feeding power is important in system designs. When calculating system leaks, it should be accepted as the ratio of daily load demand to the product of the efficiency of all units in the system. As in Equation (11), the total solar energy array (E_r) must meet the daily energy requirement.

$$E_r = \frac{E_{\text{demand}}}{\eta_{\text{sys}}}, \tag{11}$$

where E_{demand} is the required demand energy (Wh) and η_{sys} is the entire structure performance. It is necessary to make calculations in order to meet the daily energy need in the most efficient way. This value can be determined by dividing the power generation system location by the average daily sunshine duration for the region.

$$P_{\text{peak}} = \frac{E_r}{T_{\text{min}}}, \tag{12}$$

where P_{peak} is the peak energy produced from the planned photovoltaic arrays (W) and T_{min} is the least sunshine time (hours). The terms given indicate the technical characteristics of the photovoltaic array designed: module power (P_{unit}), open-circuit voltage (V_{oc}), short-circuit current (I_{sc}), maximum power point voltage (V_{mpp}), and current (I_{mpp}). The sum of photovoltaic modules (n_{PV}) can be calculated from Equation (13).

$$n_{\text{PV}} = \frac{P_{\text{peak}}}{P_{\text{unit}}}, \tag{13}$$

where n_{PV} is the sum of photovoltaic arrays andP_{unit} is the part power. The sum of photovoltaic modules includes series and sections made up of strings [54, 55]. The sum of series and strings parts can be determined from these equations:

$$\begin{aligned} n_{\text{PV(s)}} &= \frac{V_{\text{DC}}}{V_{\text{mpp}}}, \\ n_{\text{PV(p)}} &= \frac{n_{\text{PV}}}{n_{\text{PV(s)}}}, \end{aligned} \tag{14}$$

where $n_{\text{PV(s)}}$ is the sum of series parts, $n_{\text{PV(p)}}$ is the sum string of series parts, and V_{DC} is the DC link value. Most of solar projects relate to the "tilt angle" or "tilt" of a PV array or all collectors from a horizontal plane [54]. The tilt angle of a tracker plate and the tracker altitude angle are involved by the equation:

$$\text{TiltAngle} = |90\ \text{deg} - \theta_{\text{TE}}|. \tag{15}$$

The azimuth/elevation trackers work with two free cycle axes: the first is in azimuth around a vertical axis and the second is in height around a horizontal axis. The tracer azimuth can be regarded as a moving shaft at certain angles that can be geographically defined in the range of (0 degrees, 360 degrees) [56].

The SPPs shown in Figure 1 are connected to the grid and are designed to feed the charging station.

This system was designed such that the people who work in the building could charge their vehicles to full capacity during their work hours. The station's energy requirements would be continuously met with solar energy during these hours, and if needed, additional energy would be drawn from the grid.

4. System Description

The project was carried out in three buildings with the same roof sizes in Istanbul/Başakşehir, and analyses were performed using a different solar tracking system for each building. The use of the produced energy was realized with the systematic below:

(i) The designed roof-type PV energy system is connected to the grid and the energy that is produced but cannot be consumed instantaneously will be sold to the national electricity network with a bidirectional meter or it draws energy from the grid in energy requirements

(ii) The designed roof-type PV energy system primarily feeds the electric vehicle charging station

(iii) The surplus energy from the charging station is used for the lighting, ventilation, and common area energy requirements of the buildings

In this project, PV plants with 23.68 kW of DC power were installed on the roofs of three buildings with similar features in the same location. The PV plants that were mounted on these buildings comprised a fixed-angle, an adjustable-angle, and an automatic solar tracking system, each of which was realized with 320 W polycrystalline PV panels (16.5% efficiency). These systems were then monitored via energy-production data for 1 year. The projects were then compared in technical and economic terms, particularly with respect to investment and operating costs.

4.1. Annual Energy Production. Each SPP in this project was installed on the roof of a workplace in the Başakşehir District of Istanbul. The plants were installed on three separate but similar buildings in a single complex; the systems operated independently but under the same conditions and at equal power (20-kW AC output). Therefore, for the electrical project, only one of these plants will be discussed. Polycrystalline PV modules with 320 W of power and 16.5% efficiency were used in the project. A rooftop SPP with 23.68 kW of DC power and an inverter with 20 kW of AC output power were used; the system had a total of 74 modules. This power plant fueled two EV charging stations—one for big cars and one for small cars—in the building's parking lot. The system was also connected to the grid.

As can be seen in Figure 2, the actual production data are very close to the estimated production data made using PVsyst and PV*SOL software. The values in this table belong

Figure 1: The roof type SPP and its PV panels.

to SPP with fixed construction. Actual production data consists of data recorded using an inverter datalogger.

4.2. Project Layout. The project's general connection form is summarized in Figure 3. The modules convert sunlight into DC electricity, which the inverter then converts into AC at the appropriate voltage and frequency, before delivering the AC energy to the distribution panel. The panel is also connected to the grid, the building's electrical system, and EV charging station. After the panel has met the energy needs of the building and the charging station with the energy from the solar module, it transmits any surplus energy to the grid. When the solar module is insufficient (such as when there is no sunlight), the building and charging station draw power from the grid [57–67].

4.3. Power System Project. The modules were serially interconnected to form arrays. One positive output and one negative output from these arrays were then connected to the inverter. The inverter used in this project has two MPPTs (maximum power point tracker), each of which works independently. Thus, arrays of various voltage levels were connected to distinct MPPT inputs. For one MPPT input, two arrays, each with 18 modules connected in series, were connected to the inverter. For the other, two arrays, each with 19 modules connected in series, were connected to the inverter. Thus, the 74 modules (320 W) produced 23.68 kW of DC power. The output of the inverter was set to 20 kW AC. The total harmonic distortion at the output of the inverter was less than 3%.

4.4. Power Line Calculations. A TEDAŞ regulation was taken into account when calculating the inverter's compatibility with the module array; according to this regulation, the maximum cell temperature and the minimum cell temperature were 70°C and −10°C, respectively. Equations (6) and (7) were used in these calculations.

Table 1 shows the calculations for the DC voltage drop, power dissipation, and current; a 4 mm^2 cable meets all of the requirements. The k_1 and k_2 coefficients used in these calculations are the correction factors for the cables used in the project (according to the cable-laying method and the temperature). These factors were used to calculate the current that the cable can carry.

According to the regulations, 2% DC and 3% AC voltage drops are allowed. Table 2 shows the calculations for the AC voltage drop, power dissipation, and current; the chosen cables met all the requirements.

4.5. Installation Stages. Using the data from the project's implementation stages, Figure 4 shows the aluminum construction (in an unfinished state) and the SPP (once it was ready for electricity production).

An applied ergonomics analysis of the final project's solar tracking systems was also performed for use in subsequent applications. In this context, three roof-type SPPs of the same power level but with distinct tracking systems were installed. These three projects (Figure 5) had the same conditions and were part of the same building complex, and the same number and power of modules and inverters were used.

This system has higher operating and maintenance costs than the other systems because it involves rotating parts and an engine. In addition, although faults are quite rare in the other systems, engine breakdowns are common with this system. Based on tests performed by the relevant distribution company and TEDAŞ, the stations work smoothly. A grounding measurement was also performed, with a result of 1.52 Ω.

5. Results and Discussion

The results of the application project are presented and discussed below, under two headings: Electrical System Performance and Cost Analysis.

5.1. Electrical System Performance. Two different strings were formed from PV modules as 18 panels connected in series and 19 also connected in series. A total of 74 320 W PV modules were used by connecting 2 strings of 18 and 2 of 19 strings in parallel for each power plant. Strings with different voltage were connected to different MPPT inputs. This means that losses due to voltage difference were prevented and the system worked more efficiently. Simply connecting strings with the same number of serial panels to MPPT inputs is not enough to achieve this. Arrays should be created according to the similarity of the technical data in the Flash Testing Report, by looking at the serial number of the PV modules. It was observed that many applications did not pay attention to the voltage differences while creating the arrays. The researchers paid attention to this issue in this project. Furthermore, the length of the cable used in the

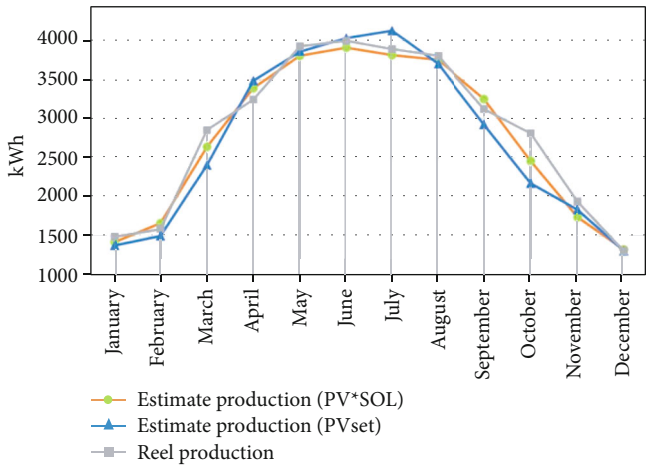

Figure 2: Estimated graph of energy injected into grid.

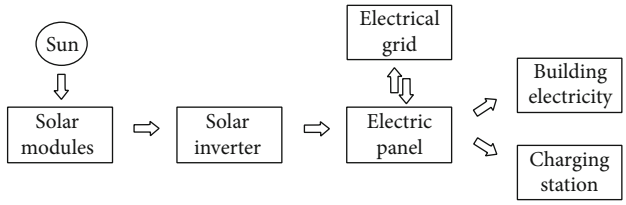

Figure 3: Project block diagram of the general arrangement.

Table 1: Calculations for the DC voltage drop (E), power dissipation, and current.

String no	L_{sum} (m)	k_1	k_2	I_o (A)	I_d (A)	P (Wp)	S (mm^2)	$\Delta v, \Delta P$ (%)
S 01	32	0.45	0.76	55	18.81	5760	4	0.188
S 02	25	0.45	0.76	55	18.81	6080	4	0.139
S 03	36	0.45	0.76	55	18.81	6080	4	0.200
S 04	60	0.45	0.76	55	18.81	5760	4	0.352

connection of the strings to the inverter is also important. The voltage drop will be different in different sizes and sections.

The total PV module power of each power plant is 23.68 kW, and the inverter output power is 20 kW. Thanks to two separate EV charging stations, each with a power of 22 kW, and a system connected to the building main panel, energy transmission losses are minimized by consuming energy on the location where it is produced. Additionally, since the power plants are connected to the grid through the building's main panel, the surplus can be transmitted to the city electricity grid. This transmission can be done smoothly with the inverters operating at the frequency and voltage compatible with the grid.

For the region where the project was conducted, data from October are roughly average with respect to sunshine and production. Accordingly, October was examined separately; Figure 6 shows the production data for the three types of power plants. The SPP with the solar tracking system produced the most energy: The fixed-angle system produced 2830.5 kWh per month, the adjustable-angle system produced 3050.4 kWh per month, and the solar-tracking system produced 3351.95 kWh per month. Based on these data, the plants with the adjustable-angle and solar tracking systems produced approximately 8% and 18% more energy, respectively, than the fixed-angle system.

There are many issues to be considered in the project implementation stages for SPPs. For example, equal numbers of voltage arrays should be connected to each MPPT when connecting the arrays to the inverter. These modules should also have test values that are as close to equal as possible so as to avoid mismatches. Attention should be paid to many factors, including the number of adjacent cables, the ambient temperature, and the method of laying the cables. The current should be determined according to these factors, and an appropriate section should be selected. Furthermore, this section should be checked for voltage drops and power dissipation. When estimating the power plants' production, attention should also be paid to time-dependent efficiency loss in the modules, as this is a general problem for semiconductors. Module manufacturers usually guarantee 80% to 85% efficiency at the end of 25 years.

A graph of the annual production data for the analysed systems (solar tracking, adjustable-angle, and fixed-angle) is presented in Figure 7.

5.2. Cost Analysis. Table 3 presents the cost of the power plants, the amount of energy production, and the return on investment, comparatively. As can be seen, the fixed system has the lowest investment and operation and maintenance cost. However, at the same time, energy generation is the lowest with this power plant. The manually adjusted system ranks second in terms of low investment cost. However, the return on investment in this power plant is observed to be the shortest. Trackers are the plants with the highest investment and operation and maintenance cost. They also achieve the highest production. However, they are still the worst plants in terms of return time. One of the reasons why the manually adjusted system works well is that technical personnel are always present at the location of the plant. This allows more frequent angle changes for the unit. Therefore, the efficiency increases by frequently adjusting the angle to the optimum. According to the results we have obtained here, the manually adjusted system is economically better. Of course, the tracker system is technically superior. The costs are gradually decreasing in the tracker system, so it will be a better choice both economically and technically in the future. If the lowest investment and operation and maintenance cost is to be preferred, a fixed system must be installed. Today, this system is more preferable due to its low cost.

Figure 8 presents the comparison of power plant production data and consumption of EV charging stations connected to this power plant. As can be seen, the power plant meets approximately 85% of the annual total consumption of the two EV charging stations. According to the EV charging station load curve used in the project, each station achieves an average of 3 hours/day EV charge annually. This demand varies depending on the number of EVs. Since the number of EVs will increase with the developing technology,

Table 2: Calculations for the AC voltage drop, power dissipation, and current.

	L (m)	S (mm^2)	k_1	k_2	k_3	I_o (A)	I_d (A)	P (We)	$\Delta v, \Delta P$ (%)
INV-R. E. panel	5	5×25	0.79	0.90	0.84	106	63.307	20000	0.045
R. E. panel-E. panel	100	5×25	0.79	0.90	0.84	106	63.307	20000	0.893
E. panel-EV 1	30	5×25	0.79	0.90	0.84	106	63.307	22170	0.297
E. panel-EV 2	25	5×16	0.79	0.90	0.84	79	47.182	11085	0.193

Figure 4: Project installation stages.

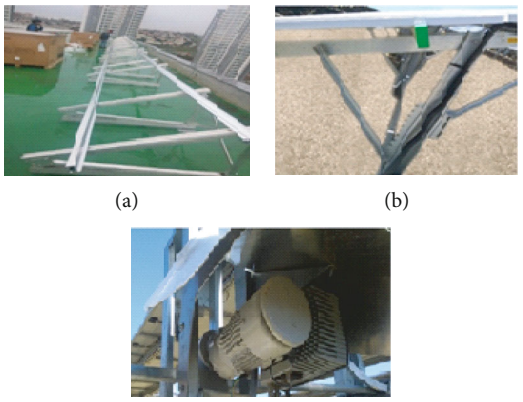

(a) (b) (c)

Figure 5: (a) PV panels for the fixed-angle, (b) manually adjustable-angle, and (c) solar tracking SPPs.

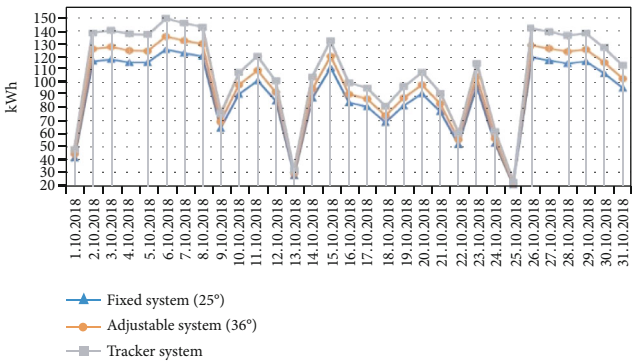

Figure 6: Comparison of October production data.

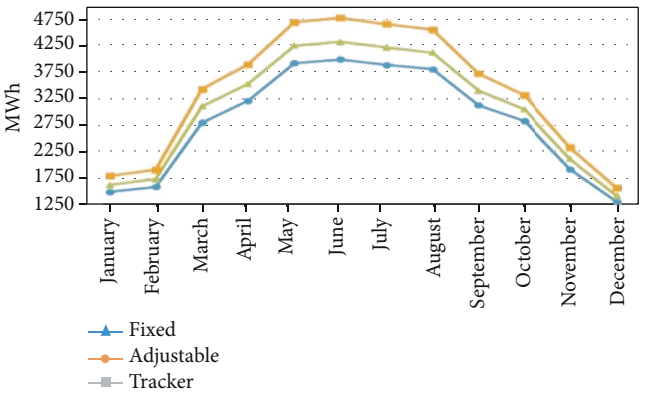

Figure 7: Graph of comparison of solar-tracking system applications according to monthly production data.

SPP power should be made as high as possible in such projects. This way, the EV charge will be achieved with clean energy as much as possible and energy transmission line losses will be minimized. Also, there may be network electrical infrastructure problems encountered, when EV charging stations draw power from the same network at the same time. To avoid this, it is recommended to install the EV charging station and SPP together just as the project in this article.

Table 3: Production costs and profits.

	Fixed	Adjustable	Tracker
Solar module	$ 7,500.00	$ 7,500.00	$ 7,500.00
Inverter	$ 2,500.00	$ 2,500.00	$ 2,500.00
DC cable	$ 200.00	$ 200.00	$ 200.00
AC cable	$ 250.00	$ 250.00	$ 250.00
Electric panel	$ 900.00	$ 900.00	$ 900.00
Workmanship	$ 2,100.00	$ 2,100.00	$ 2,100.00
Official transaction	$ 1,100.00	$ 1,100.00	$ 1,100.00
Project design	$ 2,250.00	$ 2,250.00	$ 2,250.00
Construction	$ 3,000.00	$ 4,000.00	$ 7,500.00
Other materials	$ 1,200.00	$ 1,200.00	$ 1,200.00
Unpredictable expense	$ 1,000.00	$ 1,000.00	$ 1,000.00
Total investment	$ 22,000.00	$ 23,000.00	$ 26.500.00
Produced energy	33.9 MWh/year	36.9 MWh/year	40.7 MWh/year
Annual energy sales amount	$ 4,507.89	$ 4,907.54	$ 5,409.70
Annual operation and maintenance expenses	$ 400.00	$ 500.00	$ 1,000.00
Annual yield loss	1.2%	1.2%	1.3%
Amortization time	5.75 years	5.60 years	6.31 years
10-year forecast profit	$ 16,720.91	$ 18,508.40	$ 14,539.61

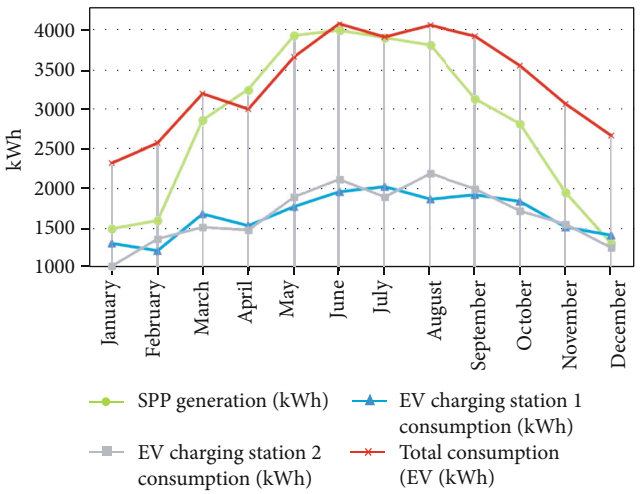

Figure 8: Graph of power plant production data and consumption of EV charging stations connected to this power plant.

According to Table 3, when accounting for the 10% loss in module efficiency over 10 years, the SPP with the fixed-angle system results in a profit of $16,720 if the electricity is sold only to the grid. This SPP does no harm to the environment because it yields profit and is a renewable energy source; it also decreases loss due to leakage because it reduces the need to transport energy to EV charging stations, as these stations can be fed without the need for an extra transmission line.

System life is 30 years, and the PV module, one of the main components used in the system, has an 80% performance guarantee at the end of 25 years. The whole system has a 10-year product and energy sale guarantee for connection to the grid. Taking into account the system life and performance loss, this power plant will save approximately 280 tons of CO_2 emission in 30 years with the energy it produces. While calculating these savings, CO_2 emissions that occur directly or indirectly during the production of all materials used and the emissions during the system's network integration are taken into account. Emission savings calculations are based on the IEA list/Turkey.

6. Conclusion

According to the annual production data for SPPs, systems with adjustable angles produced 8.4% more energy than those with fixed angles. This advantage can be further increased by changing the angle more frequently. In this project, the angles were changed four times per year. The solar tracking system also produced 19.8% more energy than the fixed-angle system. The SPPs with the solar tracking systems have higher investment, operating, and maintenance costs than the other systems, which makes the solar tracking systems less popular. The adjustable-angle and fixed-angle systems have similar costs; however, the former has much better energy production. Of the three SPPs, the one with the adjustable-angle system ranks first in terms of amortization time and 10-year earnings. With the produced power, the charge station provided energy for electric cars: either 16-A or 32-A Mode 3 alternating current. According to the EV charging station load curve used in the project, each station achieves an average of 3 hours/day EV charge annually. This demand varies depending on the number of EVs. Since the number of EVs will increase with the developing technology, SPP power should be made as high as possible in such projects.

The main purpose of this article was to demonstrate, using a real application, an optimal efficiency system analysis with low investment cost, low operating cost, and high

reliability, especially for roof applications in buildings. It was also aimed at exploring a new approach to energy-saving based on net energy gain. The main findings can be summarized as follows:

(i) In terms of energy generation, manual adjustment and single-axis solar tracking methods are the best options in the spring equinox. The E-W tracking single-axis tracking system becomes more efficient as the slope and height of the sun increase

(ii) In addition to approaches based on net energy generation, the system is also more applicable in terms of logistics, installation/operating costs, resistance to meteorological conditions, and system life

(iii) The energy consumed by the single-axis tracking system corresponds to 9.2% of the energy produced. Systems consisting of multiple components with complex designs are not always the right options

(iv) Although the single-axis tracking system is 27% more efficient than other methods of energy generation, the manually adjusted method has the shortest depreciation period

The data obtained in similar studies and the data in this project show similarities. What distinguishes this project from others is the manually adjusted system. Furthermore, projects with 3 different constructions of the same power, built using the same technical equipment at the same location, were compared. This is a guiding study for researchers who will carry out similar applications, conducted by comparing real production data and 2 different production-forecasting software estimates. Therefore, the results from this study are not only scientific work but also valuable for the green building concept, engineering, and construction (EPC) companies to make better decisions about what type of solar tracking method to use based on project details.

Nomenclature

V: Cell voltage (Volt)
V_{oc}: Cell open-circuit voltage
I_d: Reverse saturation current at the T_c temperature
I_{ph}: Photogenerated current
I_{sh}: Parallel resistor current
R_s: Series resistance
R_{sh}: Shunt resistance
T_c: Cell temperature (Kelvin)
q: Electron charge = $1.6^{*}10^{-19}$ Coulomb
K: Boltzmann constant (1.38×10^{-23} j/K)
N: Diode ideality factor
N_p: Cells in parallel
N_s: Cells in series
k_{Voc}: Temperature-dependent voltage coefficient
k_{Isc}: Temperature-dependent current coefficient
k_{Pmax}: Temperature-dependent power coefficient
t: Instantaneous cell temperature
t_{st}: Cell temperature under standard test conditions.

Data Availability

Datasets used to support the findings of this study are included within the article.

Conflicts of Interest

The authors declare that they have no conflicts of interest.

Supplementary Materials

Graphical abstract: the system was connected to the grid and electric vehicle charging station with a bidirectional energy meter to transfer the generated energy or provide the required energy. With regard to the energy production values, the automatic solar tracking system generated 10% more energy than the manually controlled system and 20% more energy than the fixed-angle system. *(Supplementary Materials)*

References

[1] S. Akshya, A. Ravindran, A. S. Srinidhi, S. Panda, and A. G. Kumar, "Grid integration for electric vehicle and photovoltaic panel for a smart home," in *Proceedings of IEEE International Conference on Circuit, Power and Computing Technologies, ICCPCT 2017*, Kollam, India, 2017.

[2] A. H. Yazdavar, M. A. Azzouz, and E. F. El-Saadany, "Modeling and simulation of standalone photovoltaic charging stations for electric vehicles," *International Journal of Computer and Information Engineering*, vol. 9, no. 1, pp. 72–80, 2015.

[3] T. Boyekin and İ. Kıyak, "Rooftop solar power plant based electric vehicle charging station," in *6. European Conference On Renewable Energy Systems (ECRES)*, Istanbul, Turkey, 2018.

[4] U. K. Das, K. S. Tey, M. Seyedmahmoudian et al., "Forecasting of photovoltaic power generation and model optimization: a review," *Renewable and Sustainable Energy Reviews*, vol. 81, Part 1, pp. 912–928, 2018.

[5] H. Kang, T. Hong, S. Jung, and M. Lee, "Techno-economic performance analysis of the smart solar photovoltaic blinds considering the photovoltaic panel type and the solar tracking method," *Energy & Buildings*, vol. 193, pp. 1–14, 2019.

[6] B. Parida, S. Iniyan, and R. Goic, "A review of solar photovoltaic technologies," *Renewable and Sustainable Energy Reviews*, vol. 15, no. 3, pp. 1625–1636, 2011.

[7] H. Hemza, C. Abdeslam, M. P. Rachid, and D. Barakel, "Tracing current-voltage curve of solar panel based on LabVIEW Arduino interfacing," *Journal of Bilişim Teknolojileri Dergisi*, vol. 8, no. 3, pp. 117–123, 2015.

[8] A. Chialastri and M. Isaacson, "Performance and optimization of a BIPV/T solar air collector for building fenestration applications," *Energy and Buildings*, vol. 150, no. 1, pp. 200–210, 2017.

[9] T. Ibn-Mohammed, S. C. L. Koh, I. M. Reaney et al., "Perovskite solar cells: an integrated hybrid lifecycle assessment and review in comparison with other photovoltaic technologies," *Renewable and Sustainable Energy Reviews*, vol. 80, pp. 1321–1344, 2017.

[10] T. D. Lee and A. U. Ebong, "A review of thin film solar cell technologies and challenges," *Renewable and Sustainable Energy Reviews*, vol. 70, pp. 1286–1297, 2017.

[11] A. C. Martins, V. Chapuis, F. Sculati-Meillaud, A. Virtuani, and C. Ballif, "Light and durable: composite structures for building-integrated photovoltaic modules," *Progress in Photovoltaics: Research and Applications*, vol. 26, no. 9, pp. 718–729, 2018.

[12] V. Ciocia, A. Boicea, A. Dematteis, P. D. Leo, F. Giordano, and F. Spertino, "PV system integration in buildings: an energy and economic case study," in *2017 10th International Symposium on Advanced Topics in Electrical Engineering (ATEE)*, Bucharest, Romania, 2017.

[13] M. Brito, S. Freitas, S. Guimarães, C. Catita, and P. Redweik, "The importance of facades for the solar PV potential of a Mediterranean city using LiDAR data," *Renewable Energy*, vol. 111, pp. 85–94, 2017.

[14] W. Bahr, "A comprehensive assessment methodology of the building integrated photovoltaic blind system," *Energy and Buildings*, vol. 82, pp. 703–708, 2014.

[15] A. Z. Hafez, A. M. Yousef, and N. M. Harag, "Solar tracking systems: technologies and trackers drive types - a review," *Renewable and Sustainable Energy Reviews*, vol. 91, pp. 754–782, 2018.

[16] S. Heslop and I. MacGill, "Comparative analysis of the variability of fixed and tracking photovoltaic systems," *Solar Energy*, vol. 107, pp. 351–364, 2017.

[17] N. AL-Rousan, N. A. M. Isa, and M. K. M. Desa, "Advances in solar photovoltaic tracking systems: a review," *Renewable and Sustainable Energy Reviews*, vol. 82, no. 3, pp. 2548–2569, 2018.

[18] M. Sorgato, K. Schneider, and R. Rüther, "Technical and economic evaluation of thin-film CdTe building-integrated photovoltaics (BIPV) replacing façade and rooftop materials in office buildings in a warm and sunny climate," *Renewable Energy*, vol. 118, pp. 84–98, 2018.

[19] A. Vulkan, I. Kloog, M. Dorman, and E. Erell, "Modeling the potential for PV installation in residential buildings in dense urban areas," *Energy and Buildings*, vol. 169, pp. 97–109, 2018.

[20] A. K. Athienitis, G. Barone, A. Buonomano, and A. Palombo, "Assessing active and passive effects of façade building integrated photovoltaics/thermal systems: dynamic modelling and simulation," *Applied Energy*, vol. 209, pp. 355–382, 2018.

[21] A. Yushchenko, A. de Bono, B. Chatenoux, M. K. Patel, and N. Ray, "GIS-based assessment of photovoltaic (PV) and concentrated solar power (CSP) generation potential in West Africa," *Renewable and Sustainable Energy Reviews*, vol. 81, no. 2, pp. 2088–2103, 2018.

[22] R. Singh, S. Kumar, A. Gehlot, and R. Pachauri, "An imperative role of sun trackers in photovoltaic technology: a review," *Renewable and Sustainable Energy Reviews*, vol. 82, no. 3, pp. 3263–3278, 2018.

[23] M. Tripathy, P. Sadhu, and S. Panda, "A critical review on building integrated photovoltaic products and their applications," *Renewable and Sustainable Energy Reviews*, vol. 61, pp. 451–465, 2016.

[24] J.-Y. Kim, G.-Y. Jeon, and W.-H. Hong, "The performance and economical analysis of grid-connected photovoltaic systems in Daegu, Korea," *Applied Energy*, vol. 86, no. 2, pp. 265–272, 2009.

[25] Y. Kim, H. Cha, B.-M. Song, and K. Y. Lee, "Design and control of a grid-connected three-phase 3-level NPC inverter for building integrated photovoltaic systems," in *PES Innovative Smart Grid Technologies (ISGT)*, Washington, DC, USA, 2012.

[26] M. Mandalaki, T. Tsoutsos, and N. Papamanolis, "Integrated PV in shading systems for Mediterranean countries: balance between energy production and visual comfort," *Energy and Buildings*, vol. 77, pp. 445–456, 2014.

[27] W. Zhang, L. Lu, and J. Peng, "Evaluation of potential benefits of solar photovoltaic shadings in Hong Kong," *Energy*, vol. 137, pp. 1152–1158, 2017.

[28] M. Mandalaki, S. Papantoniou, and T. Tsoutsos, "Assessment of energy production from photovoltaic modules integrated in typical shading devices," *Sustainable Cities and Society*, vol. 10, pp. 222–231, 2014.

[29] C. Vassiliades, A. Michael, A. Savvides, and S. Kalogirou, "Improvement of passive behaviour of existing buildings through the integration of active solar energy systems," *Energy*, vol. 163, pp. 1178–1192, 2018.

[30] C. Breyer, D. Bogdanov, A. Gulagi et al., "On the role of solar photovoltaics in global energy transition scenarios," *Progress in Photovoltaics: Research and Applications*, vol. 25, no. 8, pp. 727–745, 2017.

[31] J. Oh, C. Koo, T. Hong, K. Jeong, and M. Lee, "An economic impact analysis of residential progressive electricity tariffs in implementing the building-integrated photovoltaic blind using an advanced finite element model," *Applied Energy*, vol. 202, pp. 259–274, 2017.

[32] Y. Chen, P. Xu, J. Gu, F. Schmidt, and W. Li, "Measures to improve energy demand flexibility in buildings for demand response (DR): a review," *Energy and Buildings*, vol. 177, pp. 125–139, 2018.

[33] N. X. Truong, N. L. Tung, N. Q. Hung, and B. Delinchant, "Grid-connected PV system design option for nearly zero energy building in reference building in Hanoi," in *International Conference on Sustainable Energy Technologies (ICSET)*, Hanoi, Vietnam, 2016.

[34] A. Chub, O. Korkh, R. Kosenko, and D. Vinnikov, "Novel approach immune to partial shading for photovoltaic energy harvesting from building integrated PV (BIPV) solar roofs," in *20th European Conference on Power Electronics and Applications (EPE'18 ECCE Europe)*, Riga, Latvia, 2018.

[35] İ. Kıyak, B. Oral, and V. Topuz, "Smart indoor LED lighting design powered by hybrid renewable energy systems," *Energy and Buildings*, vol. 148, pp. 342–347, 2017.

[36] TEDAŞ, *Turkey electricity distribution company*, Technical Report, Turkey, 2018.

[37] BEDAŞ, *Boğaziçi electricity distribution company*, Technical Report, Istanbul, Turkey, 2018.

[38] K. Jeong, T. Hong, C. Koo, J. Oh, M. Lee, and J. Kim, "A prototype design and development of the smart photovoltaic system blind considering the photovoltaic panel, tracking system, and monitoring system," *Applied Sciences*, vol. 7, no. 10, p. 1077, 2017.

[39] E. Taveres-Cachat, K. Bøe, G. Lobaccaro, F. Goia, and S. Grynning, "Balancing competing parameters in search of optimal configurations for a fix louvre blade system with integrated PV," *Energy Procedia*, vol. 122, pp. 607–612, 2017.

[40] C. Koo, T. Hong, K. Jeong, C. Ban, and J. Oh, "Development of the smart photovoltaic system blind and its impact on net-zero energy solar buildings using technical-economic-political analyses," *Energy*, vol. 124, pp. 382–396, 2017.

[41] M. Macellari, U. Grasselli, and L. Schirone, "Modular MPPT converter with series-connection for PV installations embedded in the urban environment," in *IECON 2013-39th Annual*

Conference of the IEEE Industrial Electronics Society, Vienna, Austria, 2013.

[42] B. H. Lim, C. S. Lim, H. Li et al., "Industrial design and implementation of a large-scale dual-axis sun tracker with a vertical-axis-rotating-platform and multiple-row-elevation structures," *Solar Energy*, vol. 199, pp. 596–616, 2020.

[43] X. C. Ngo, T. H. Nguyen, N. Y. Do et al., "Grid-connected photovoltaic systems with single-axis sun tracker: case study for Central Vietnam," *Energies*, vol. 13, no. 6, article 1457, 2020.

[44] O. Achkari, A. El Fadar, I. Amlal, A. Haddi, M. Hamidoun, and S. Hamdoune, "A new sun-tracking approach for energy saving," *Renewable Energy*, vol. 169, pp. 820–835, 2021.

[45] H. Allamehzadeh, "An update on solar energy and sun tracker technology with a dual axis sun tracker application," in *2019 IEEE 46th Photovoltaic Specialists Conference (PVSC)*, Chicago, IL, USA, 2019.

[46] M. G. Satué, F. Castaño, M. G. Ortega, and F. R. Rubio, "Auto-calibration method for high concentration sun trackers," *Solar Energy*, vol. 198, pp. 311–323, 2020.

[47] G. Li, Q. Xuan, M. W. Akram, Y. G. Akhlaghi, H. Liu, and S. Shittu, "Building integrated solar concentrating systems: a review," *Applied Energy*, vol. 260, article 114288, 2020.

[48] P. Hoseinzadeh, M. K. Assadi, S. Heidari et al., "Energy performance of building integrated photovoltaic high-rise building: case study, Tehran, Iran," *Energy and Buildings*, vol. 235, article 110707, 2021.

[49] T. E. Kuhn, C. Erban, M. Heinrich, J. Eisenlohr, F. Ensslen, and D. H. Neuhaus, "Review of technological design options for building integrated photovoltaics (BIPV)," *Energy and Buildings*, vol. 231, article 110381, 2021.

[50] A. Awasthi, A. K. Shukla, S. R. Murali Manohar et al., "Review on sun tracking technology in solar PV system," *Energy Reports*, vol. 6, pp. 392–405, 2020.

[51] J. E. Gonçalves, T. van Hooff, and D. Saelens, "Simulating building integrated photovoltaic facades: comparison to experimental data and evaluation of modelling complexity," *Applied Energy*, vol. 281, p. 116032, 2021.

[52] S. Abdallah and O. O. Badran, "Sun tracking system for productivity enhancement of solar still," *Desalination*, vol. 220, no. 1-3, pp. 669–676, 2008.

[53] I. H. Rosma, J. Asmawi, S. Darmawan, B. Anand, N. D. Ali, and B. Anto, "The implementation and analysis of dual axis sun tracker system to increase energy gain of solar photovoltaic," in *2018 2nd International Conference on Electrical Engineering and Informatics (ICon EEI)*, Batam, Indonesia, 2018.

[54] T. F. Megahed and A. Radwan, "Performance investigation of zero-building-integrated photovoltaic roof system: a case study in Egypt," *Alexandria Engineering Journal*, vol. 59, no. 6, pp. 5053–5067, 2020.

[55] C. D. Rodríguez-Gallegos, O. Gandhi, S. K. Panda, and T. Reindl, "On the PV tracker performance: tracking the sun versus tracking the best orientation," *IEEE Journal of Photovoltaics*, vol. 10, no. 5, pp. 1474–1480, 2020.

[56] D. Riley and C. Hansen, "Sun-relative pointing for dual-axis solar trackers employing azimuth and elevation rotations," *Journal of Solar Energy Engineering*, vol. 137, no. 3, article 031008, 2015.

[57] X. Jiang, J. Wang, Y. Han, and Q. Zhao, "Coordination dispatch of electric vehicles charging/discharging and renewable energy resources power in microgrid," *Procedia Computer Science*, vol. 107, pp. 157–163, 2017.

[58] M. Clemente, M. P. Fanti, and W. Ukovich, "Smart management of electric vehicles charging operations: the vehicle-to-charging station assignment problem," in *19th World Congress The International Federation of Automatic Control*, Cape Town, South Africa, 2014.

[59] W. Shengjun, X. Qingshan, L. Qun, Y. Xiaodong, and C. Bing, "Optimal EV charging control strategy based on DC microgrid," *Energy Procedia*, vol. 100, pp. 243–247, 2016.

[60] Ö. Polat, K. Yumak, M. S. Sezgin, G. Yumurtaci, and Ö. Gül, "Elektrikli Araç Ve Şarj İstasyonlarının Türkiye'deki Güncel Durumu," in *VI. Energy Efficiency, Quality Symposium and Exhibition, EVK'2015*, Kocaeli, Turkey, 2015.

[61] S o A, *Engineers, SAE J1772- Electric Vehicle and Plug in Hybrid Electric Vehicle Conductive Charge Coupler*, 2012.

[62] IE Commission, *IEC 61851-1- Electric Vehicle Conductive Charging System - Part 1: General Requirements*, 2011.

[63] C Association, *Technical Specifications of Quick Charger for the Electric Vehicle*, 2011.

[64] B. Yağcıtekin, M. Uzunoğlu, and A. Karakaş, "A new deployment method for electric vehicle charging infrastructure," *Turkish Journal of Electrical Engineering and Computer Sciences*, vol. 24, no. 3, pp. 1292–1305, 2016.

[65] M. Brenna, M. Longo, and W. Yaïci, "Modelling and simulation of electric vehicle fast charging stations driven by high speed railway systems," *Energies*, vol. 10, no. 9, p. 1268, 2017.

[66] B. Zhao, M. Hu, X. Ao et al., "A novel strategy for a building-integrated diurnal photovoltaic and all-day radiative cooling system," *Energy*, vol. 183, pp. 892–900, 2019.

[67] C. Ghenai and M. Bettayeb, "Modelling and performance analysis of a stand-alone hybrid solar PV/fuel cell/diesel generator power system for university building," *Energy*, vol. 171, pp. 180–189, 2019.